Inflammation, Vol. 38, No. 1, February 2015 (© 2014)
DOI: 10.1007/s10753-014-0031-y

NS5ATP9 Suppresses Activation of Human Hepatic Stellate Cells, Possibly via Inhibition of Smad3/Phosphorylated-Smad3 Expression

Mengran Zhang,[1,2] Jinqian Zhang,[1,2] Shunai Liu,[1,2] Qi Wang,[1,2] Guoxian Lin,[3] Rongxian Qiu,[3] Min Quan,[2] and Jun Cheng[1,2,4]

Abstract—Activation of hepatic stellate cell (HSC) is the central event in liver fibrosis. NS5ATP9 is related to many malignant tumors, but little is known about its function in HSC activation. The aim of this study is to investigate the role of NS5ATP9 in HSC activation *in vitro*. Genes related to liver fibrosis were detected after NS5ATP9 overexpression or silencing with or without transforming growth factor (TGF)-β1 stimulation in the human HSCs by real-time polymerase chain reaction and western blotting. Cell proliferation, migration, and apoptosis were tested, and the mechanisms underlying the effect of NS5ATP9 on HSC activation were studied. We showed that NS5ATP9 suppressed HSC activation and collagen production, with or without TGF-β1 induction. Also, NS5ATP9 inhibited cell proliferation and migration and promoted apoptosis. Furthermore, NS5ATP9 reduced basal and TGF-β1-mediated Smad3/phosphorylated-Smad3 expression. The existence of a physical complex between NS5ATP9 and Smad3 was illustrated. NS5ATP9 suppresses HSC activation, extracellular matrix production, and promotes apoptosis, in part through reducing Smad3/phosphorylated-Smad3 expression.

KEY WORDS: NS5ATP9; liver fibrosis; LX-2 cells; TGF-β1; extracellular matrix.

INTRODUCTION

Liver fibrosis is caused by chronic liver injuries, which trigger hepatocyte apoptosis, endothelial barrier damage, inflammatory cell recruitment, increased transforming growth factor (TGF)-β1 secretion, and stimulation of pathways that regulate fibrosis regression and activation of myofibroblasts responsible for scar formation [1, 2]. To date, there is no effective treatment for liver fibrosis, and therefore, identification of the molecular targets for liver fibrosis treatment is necessary.

Following hepatic injury, hepatic stellate cell (HSC), the key fibrogenic cell in liver fibrosis, becomes activated, proliferates, migrates, and produces the extracellular matrix (ECM) [3]. Moreover, the transforming growth factor TGF-β1/Smad3 signal pathway plays a prominent role in wound healing and organ fibrogenesis and can activate HSC and promote collagen synthesis [4–6]. Therefore, blocking of the TGF-β1/Smad3 signaling pathway might be a potential and effective therapeutic strategy against fibrogenesis.

The gene for NS5ATP9 (HCV NS5A-transactivated protein 9), also known as KIAA0101, p15 (PAF), L5, or OEACT-1 (GenBank accession no. AF529370), is located at 15q22.1, is 336-bp long, and encodes a 111-residue protein. The gene product of NS5ATP9 was originally identified as a proliferating cell nuclear antigen-binding protein by a yeast two-hybrid assay [7] and as a target gene

Mengran Zhang and Jinqian Zhang contributed equally to this work

Electronic supplementary material The online version of this article (doi:10.1007/s10753-014-0031-y) contains supplementary material, which is available to authorized users.

[1] Institutes of Infectious Diseases, Beijing Ditan Hospital, Capital Medical University, 8 East Jingshun St., Beijing, 100015, China
[2] Beijing Key Laboratory of Emerging Infectious Diseases, Beijing, 100015, China
[3] Department of Infectious Disease, Affiliated Hospital of Putian College, Fujian, 351100, China
[4] To whom correspondence should be addressed at Beijing Key Laboratory of Emerging Infectious Diseases, Beijing, 100015, China. E-mail: jun.cheng.ditan@gmail.com

transactivated by the hepatitis C virus (HCV) NS5A protein via the suppression subtractive hybridization technique by our group [8]. NS5ATP9 expression was significantly altered in numerous malignant tumors, including pancreatic cancer, colorectal adenoma and adenocarcinoma, non-small cell lung cancer, anaplastic thyroid carcinoma, and liver cancer [9–13]. NS5ATP9 is also involved in the regulation of DNA repair, apoptosis, cellular signaling pathway, cell cycle progression, and cell proliferation [11, 14, 15]. Our recent study on NS5ATP9 showed that NS5ATP9 regulates the function of beclin 1 and participates in autophagy in cells with HCV infection [16]. Moreover, our DNA microarray data obtained by either overexpressing or silencing NS5ATP9 showed differing expression of liver fibrosis-related genes in hepatocytes (Wang Q, unpublished data), which indicated that NS5ATP9 might be related to liver fibrosis. Furthermore, we analyzed NS5ATP9 expression in the liver biopsy tissue of patients with liver fibrosis by immunohistochemistry and found that NS5ATP9 was expressed not only in hepatocytes but also in mesenchymal cells (data not shown). This further suggested that NS5ATP9 might have effects on HSCs. However, its role in liver fibrosis or HSC activation has not yet been studied. Therefore, it would be interesting to determine its role in HSC activation.

MATERIALS AND METHODS

Cell Culture, Transfection, and Treatment

LX-2 cells (human HSC cell line) were purchased from Xiang Ya Central Laboratory (Xiang Ya School of Medicine, China). HepG2 and L02 cell lines were purchased from American Type Culture Collection (Manassas, VA, USA). All cells were maintained in Dulbecco's modified Eagle's medium (DMEM) supplemented with 10 % fetal bovine serum (FBS). Cell transfection was performed with the PolyPlus-transfection reagent (n°06Y0312E9; PolyPlus-transfection SA, NY, USA). Human recombinant TGF-β1 from R&D Systems Inc. (240-B-010/CF; Minneapolis, MN, USA) was added to the supernatant at 2.5 or 5 ng/mL for 24 h as previously described [17, 18].

Plasmid Construction

The human NS5ATP9 gene was amplified and inserted into the vector pcDNA3.1/myc-His(−), as described by Quan M *et al.* [16].

Short Interfering RNA (siRNA) Oligonucleotides

siRNA duplexes against human NS5ATP9 and a negative control siRNA were purchased from Invitrogen (NY, USA) as described by Quan M *et al.* [16].

RNA Isolation and Quantitative Real-Time PCR (Real-Time qPCR)

RNA was extracted according to the manufacturer's instructions using the Total RNA Kit (R6834, Omega, GA, USA) and analyzed by quantitative PCR using SYBR Green qPCR Master Mix (1206352, Applied Biosystems, Warrington, UK) on an ABI 7500 System (Applied Biosystems, NY, USA). The optimized primers used for real-time PCR are listed in Table 1.

Western Blotting and Antibodies

Cells were lysed and the protein concentration was determined by the Pierce BCA assay (23225; Thermo Scientific, PA, USA). Polyvinylidene fluoride membranes were reacted with primary antibodies such as anti-NS5ATP9 (ab56773; Abcam), anti-α-smooth muscle actin (SMA) (BM0002; Boster, Wuhan, China), anti-collagen I (ab84956; Abcam), anti-collagen III (ab7778; Abcam), anti-Smad3 (9523; CST), anti-p-Smad3 (9520; CST), and anti-GAPDH (5174; CST).

Proliferation Assay

LX-2 cells were seeded into a 96-well plate and deprived of serum for 24 h before the experiment. Cell Counting Kit-8 (CCK8) solution (EQ645; DOJINDO, Kumamoto, Japan) was added to each well and the optical density was read at 450 nm according to the manufacturer's instructions.

Table 1. Primers Used for Real-Time Polymerase Chain Reaction (PCR)

Genes	Sense (5′–3′)	Antisense (5′–3′)
Human α-SMA	gggaatgggacaaaaagaca	cttcaggggcaacacgaa
Human TGF-β1	cacgtggagctgtaccagaa	cagccggttgctgaggta
Human Smad3	caccacgcagaacgtcaa	gatgggacacctgcaacc
Human Collagen1A1	gggattccctggacctaaag	ggaacacctcgctctcca
Human Collagen1A2	ctggagaggctggtactgct	agcaccaagaagaccctgag
Human Collagen3A1	ctggaccccagggtcttc	gaccatctgatccagggtttc

Migration Assay

The migratory capacity of LX-2 cells was investigated using the Millicell Hanging Cell Culture 24-well PET 8 μm (Millipore, MA, USA) placed in the well of a 24-well cell culture plate. In these experiments, 0.9 mL of DMEM/10 % FBS was added to the lower chamber of the well, and LX-2 cells transfected with NS5ATP9-specific plasmid or siRNA for 48 h were suspended in 0.2 mL of FBS-free DMEM medium and added to the upper chamber (5,000 cells per chamber). After 24 h of incubation, the culture medium was removed, and cells adhering to the membrane were fixed with 10 % formalin and stained with crystal violet solution. The total number of LX-2 cells and the number of LX-2 cells on the lower surface were counted in five microscopic fields randomly chosen for each specimen using a Nikon Eclipse TS-100 microscope, respectively.

Flow Cytometry

Cells were treated with the Annexin V-FITC/7-AAD apoptosis detection kit (640906/420404; BioLegend, CA, USA) according to the manufacturer's protocol and were analyzed via flow cytometry (Epics Altra II; Beckman Coulter, CA, USA).

Co-immunoprecipitation (co-IP)

The total proteins of the LX-2 cells, L02 cells, and HepG2 cells were lysed in radio immunoprecipitation assay buffer. Lysates were incubated overnight with NS5ATP9 antibody before being absorbed with protein A/G PLUS-agarose beads (sc-2003; Santa Cruz Biotechnology). The precipitated immunocomplexes were prepared for western blotting.

Immunofluorescence Imaging

As previously described [18], cells grown on the coverslips were fixed in 4 % paraformaldehyde and stained with anti-NS5ATP9 (1:50, sc-65162; Santa Cruz Biotechnology) and anti-Smad3 (1:00, 9523; CST) antibodies, followed by fluorescein isothiocyanate (FITC)- and tetramethylrhodamine isothiocyanate-conjugated secondary antibodies using standard procedures. Nuclei were stained with 4′,6-diamidino-2-phenylindole (DAPI, D9542; Sigma-Aldrich), followed by analysis with confocal microscopy (LSM510Meta; Zeiss, Germany).

Statistical Analysis

Statistical evaluation for data analysis was determined using the paired Student's t test. The data were obtained from at least three independent trials. All data are shown as mean±standard deviation (SD). SPSS 17.0 software (SPSS Inc., Chicago, IL, USA) was used for statistical analysis. A statistical difference of $P < 0.05$ was considered significant.

RESULTS

The Expression of NS5ATP9 in LX-2 Cells With or Without TGF-β1 Stimulation

We observed that NS5ATP9 was expressed in LX-2 cells with a mild-to-moderate level (Fig. 1). Also, the stimulation of activated HSCs by TGF-β1 is believed to be the key fibrogenic response in liver fibrosis. LX-2 cells can be further activated by TGF-β1 [19–21]. Therefore, we used human recombinant TGF-β1 protein to treat LX-2 cells and then examined the expression level of NS5ATP9. We found that the protein level of NS5ATP9 was markedly enhanced after TGF-β1 stimulation for 24 h in a dose-dependent manner (Fig. 1). Meanwhile, we observed a similar increase in α-SMA, collagen type I (COLI), and collagen type III (COLIII) levels and confirmed that TGF-β1 could stimulate further LX-2 cell activation. Also, we found that Smad3 expression decreased with TGF-β1 stimulation (Figs. 1 and 2g, h).

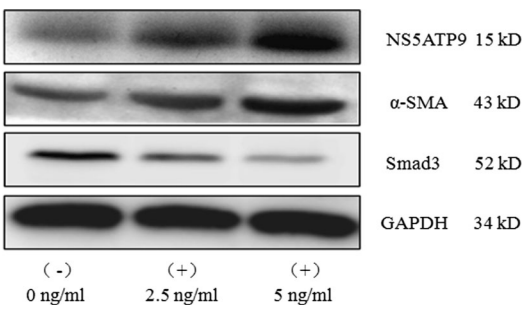

Fig. 1. The expression of NS5ATP9 in LX-2 cells with or without TGF-β1 stimulation. LX-2 cells were treated with increasing doses of human recombinant TGF-β1 (0, 2.5, and 5 ng/mL) for 24 h, and then the cells were collected to assess NS5ATP9, α-SMA, and Smad3 expression levels by western blotting. TGF-β1 stimulation upregulated the expression levels of NS5ATP9 and α-SMA in a dose-dependent manner but downregulated Smad3 expression. The quantitative ratios are shown as relative optical densities of the bands normalized to GAPDH expression. The data are representative of three independent experiments.

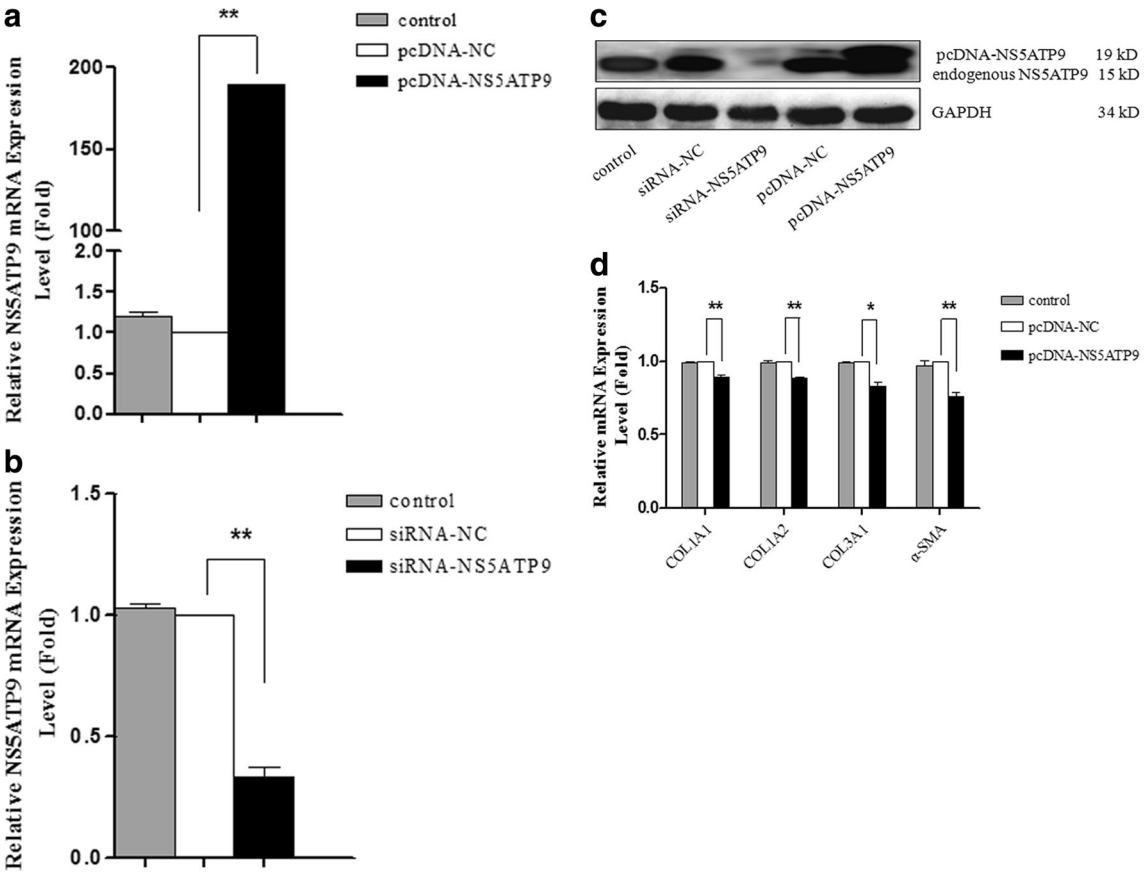

Fig. 2. NS5ATP9 suppressed basal/TGF-β1-induced ECM production and HSC activation in LX-2 cells. LX-2 cells were transfected transiently with pcDNA 3.1/myc-His(−)-NS5ATP9 plasmid or siRNA-NS5ATP9 for 48 h. pcDNA3.1/myc-His(−) and siRNA-NC were used as the respective negative controls, and the non-transfected LX-2 cells were used as the blank control. The expression of NS5ATP9 and efficiency of RNA interference were analyzed at the mRNA level (**a**, **b**) and protein level (**c**) via real-time PCR and western blotting. **d** Real-time PCR analysis showed that the levels of COL1A1, COL1A2, COL3A1, and α-SMA mRNA were significantly downregulated by NS5ATP9 overexpression, **e** while they were significantly upregulated after NS5ATP9 silencing. **f** The protein expression levels of COLI, COLIII, and α-SMA decreased dramatically after LX-2 cells were induced to express NS5ATP9, while they increased after NS5ATP9 silencing. On the other hand, after 24 h of transfection of cells according to the above method, the medium was replaced with serum-free medium in the presence or absence of TGF-β1 (5 ng/mL) and the cells were incubated for an additional 24 h before harvesting. **g**, **h** The levels of COL I, COL III, and α-SMA were measured by western blotting. β-Actin was used as the internal control in real-time PCR. The quantitative ratios are shown as relative optical densities of the bands normalized to GAPDH expression. The western blotting data were quantified by using Bio1D software (VILBER, S:11.640150, France). The results shown are mean±SD. All assays were performed in triplicates. $*P<0.05$, $**P<0.01$.

NS5ATP9 Suppressed Basal/TGF-β1-Induced ECM Production and HSC Activation in LX-2 Cells

NS5ATP9 overexpression and knockdown were achieved in LX-2 cells by introducing plasmids and siRNA, respectively. pcDNA3.1/myc-His(−)-NS5ATP9 (pNS5ATP9) and the control vector pcDNA3.1/myc-His(−) (pNC) were transiently transfected into LX-2 cells. After 48 h, NS5ATP9 was successfully overexpressed and detected by real-time qPCR (Fig. 2a) and western blotting (Fig. 2c). Furthermore, siRNA was used to silence endogenous NS5ATP9, and its successful silencing was verified using the same methods (Fig. 2b, c).

To evaluate the effect of NS5ATP9 on HSC activation, we analyzed the mRNA levels of 30 genes related to liver fibrosis, including COL I, COLIII, and α-SMA, by real-time qPCR after the overexpression or silencing of NS5ATP9 in LX-2 cells (Supporting Fig. S1). We found that NS5ATP9 overexpression downregulated the mRNA levels of collagen type I α1 (COL1A1), collagen type I α2 (COL1A2), collagen type III α1 (COL3A1), and α-SMA

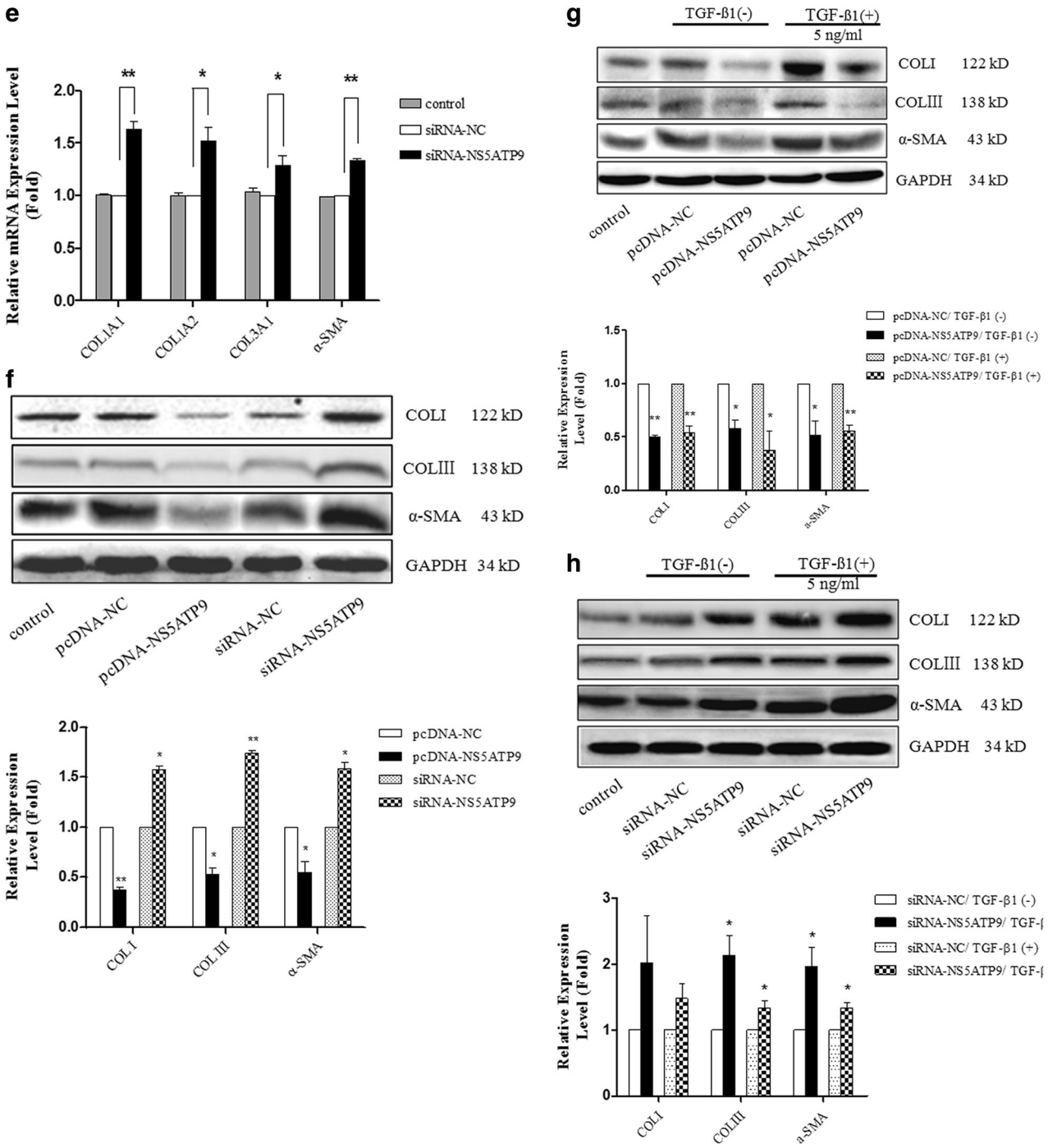

Fig. 2. (continued)

(Fig. 2d), while NS5ATP9 silencing resulted in the reverse effect (Fig. 2e). We further detected the protein levels of these genes by western blotting and observed similar effects (Fig. 2f).

Moreover, NS5ATP9 overexpression abrogated TGF-β1-induced increase in COL I, COL III, and α-SMA levels in LX-2 cells, whereas NS5ATP9 silencing coordinated with TGF-β1 to promote their expression (Fig. 2g, h).

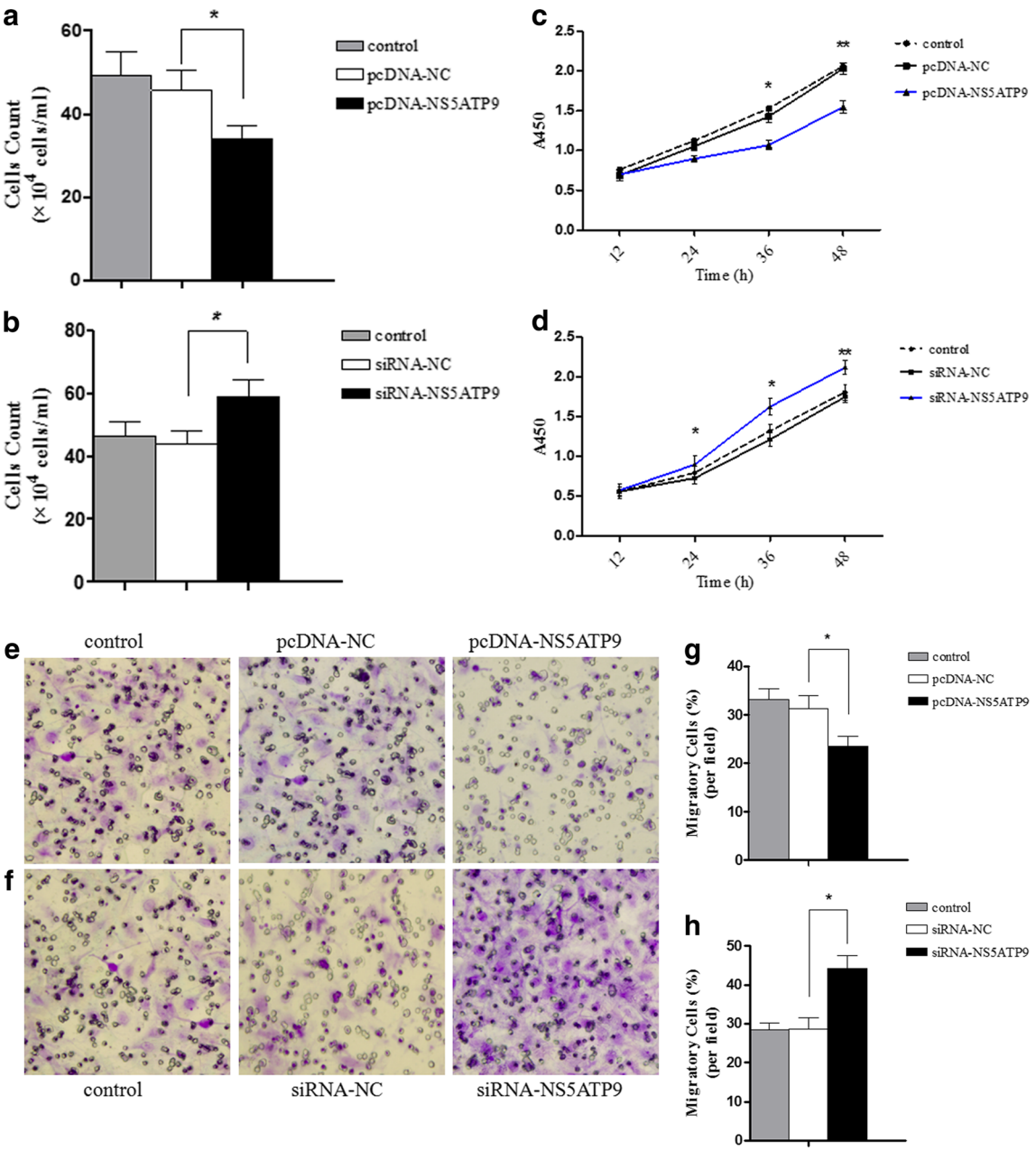

Fig. 3. NS5ATP9 inhibited LX-2 cell proliferation and migration. LX-2 cells were transiently transfected with pcDNA3.1/myc-His(-)-NS5ATP9 (pcDNA3.1/myc-His(-) as the negative control) or siRNA-NS5ATP9 (siRNA-NC as the negative control), and the non-transfected LX-2 cells were used as the blank control. Then, the proliferation and migration ability of the cells were measured with CCK8 kit and transwell assay, respectively. **a** The cell number decreased after transfection with pcDNA-NS5ATP9 for 48 h (n=5). **b** The cell number increased after transfection with siRNA-NS5ATP9 for 48 h (n=5). **c**, **d** The growth curves of LX-2 showed that NS5ATP9 upregulation inhibited cell proliferation, while its downregulation promoted proliferation (n=5). **e**, **g** The rate of migratory cells (the number of migratory cells/the total number of cells at the time of detection) dramatically decreased compared to that for the control vector group after NS5ATP9 overexpression for 48 h (n=3). **f**, **h** The rate of migratory cells dramatically increased compared to that for the siRNA-NC group after NS5ATP9 knockdown for 48 h (n=3). All the data are shown as the mean±SD. pcDNA-NS5ATP9 versus pcDNA-NC or siRNA-NS5ATP9 versus siRNA-NC, *P<0.05, **P<0.01.

NS5ATP9 Inhibited LX-2 Cell Proliferation and Migration

Proliferation and migration are the key behavioral changes in HSCs in a sustained activation state. After overexpressing NS5ATP9 in LX-2 cells by transfection with pNS5ATP9 for 48 h, we observed that the cell number was far less than that of the negative control group (Fig. 3a) and that the reverse phenomenon occurred in NS5ATP9-silenced cells (Fig. 3b). Therefore, we explored the effect of NS5ATP9 on LX-2 cell proliferation by using the CCK8 proliferation assay. NS5ATP9 overexpression significantly inhibited the growth rate of LX-2 cells compared to that of the control vector cells (Fig. 3c) and siNS5ATP9 cells showed a much faster growth rate than the silencing negative control (siNC) cells (Fig. 3d). Moreover, the effects of NS5ATP9 on the migration of LX-2 cells were further evaluated, with the migration percentage of NS5ATP9-overexpressing cells and the control vector cells being 23.5 % and 31.2 %, respectively ($P<0.05$) (Fig. 3e, g). On the contrary, knockdown NS5ATP9 significantly improved the migration ability of LX-2 cells, with the percentage of migratory siNS5ATP9 and siNC cells being 44.2 % and 28.6 %, respectively ($P<0.05$) (Fig. 3f, h).

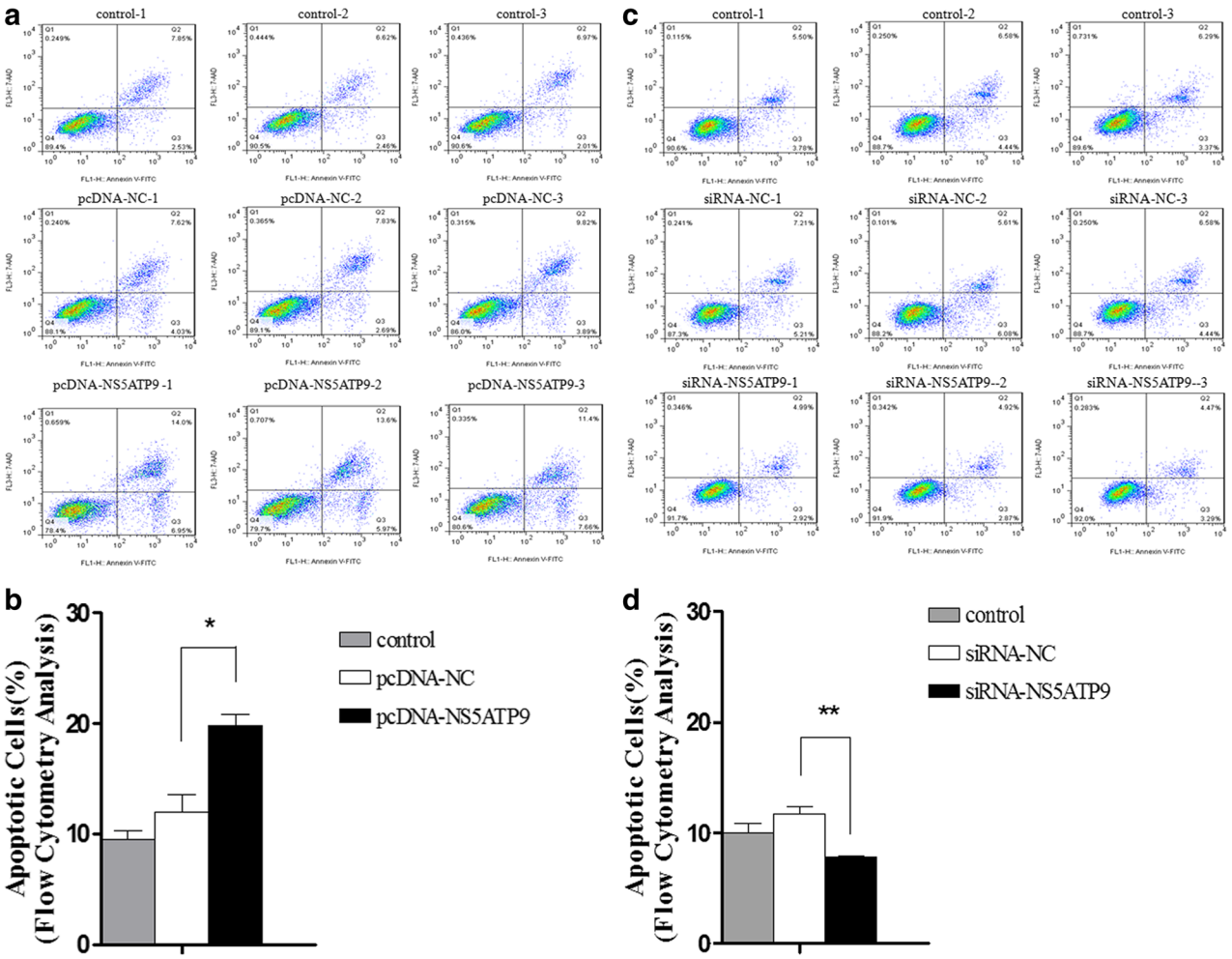

Fig. 4. NS5ATP9 promoted LX-2 cell apoptosis. LX-2 cells were transiently transfected with pcDNA3.1/myc-His(-)-NS5ATP9 (pcDNA3.1/myc-His(-) as the negative control) or siRNA-NS5ATP9 (siRNA-NC as the negative control) for 48 h, and the non-transfected LX-2 cells were used as the blank control. Then, the apoptosis rates of the cells were measured using Annexin V-FITC/7-AAD by flow cytometry. **a**, **b** The apoptosis rate dramatically increased compared to that for the control vector group after NS5ATP9 overexpression for 48 h. **c**, **d** The apoptosis rate dramatically decreased compared to that for the siRNA-NC group after NS5ATP9 knockdown for 48 h. All the data are shown as the mean±SD. All assays were performed in triplicates. *$P<0.05$.

NS5ATP9 Promoted LX-2 Cell Apoptosis

Apoptosis of activated HSCs has been considered an important mechanism of cellular clearance during fibrosis resolution [22]. To further investigate the function of NS5ATP9 in apoptosis, the apoptosis rates were measured by flow cytometry analysis. The percentage of apoptosis in the NS5ATP9-overexpressing cells was significantly higher than that of the control vector cells (Fig. 4a), with the average percentage of apoptotic pNS5ATP9 and pNC cells being 19.9 % and 12.0 %, respectively ($P<0.05$) (Fig. 4b). Moreover, the percentage of apoptosis of siNS5ATP9 cells was significantly lower than that of the control cells (Fig. 4c), with the average percentage of apoptotic siNS5ATP9 and siNC cells being 7.8 % and 11.7 %, respectively ($P<0.05$) (Fig. 4d).

NS5ATP9 Inhibited Basal Smad3/P-Smad3 Expression and Abrogated TGF-β1-Mediated P-Smad3 Increase in LX-2 Cells

We found that NS5ATP9 overexpression downregulated the mRNA levels of Smad3 and TGF-β1 (Fig. 5a), while NS5ATP9 silencing resulted in the reverse effect (Fig. 5b) in LX-2 cells. Also, at the protein level, we observed the same result in Smad3, but not in TGF-β1 (Fig. 5c). Because phosphorylated Smad3 (p-Smad3) is the central mediator of the TGF-β signaling pathway [23, 24], we added it as another detection index. We further detected the protein expression of p-Smad3 and observed similar effects (Fig. 5c). Indeed, TGF-β1 could induce Smad3 phosphorylation (Fig. 5d, e). In addition, we found that NS5ATP9 overexpression abrogated TGF-β1-mediated p-Smad3 increase, whereas NS5ATP9 silencing coordinated with TGF-β1 to promote its expression (Fig. 5d, e).

NS5ATP9 Interacts with Smad3 in LX-2 Cells

The mechanism underlying NS5ATP9-mediated regulation of the TGF-β1/Smad3 signal transduction pathway remains unclear. Therefore, to investigate if there is a protein–protein interaction between NS5ATP9 and Smad3, we performed a yeast two-hybrid screening of a human liver cDNA library by using full-length NS5ATP9 as bait. Screening 4 million transformants helped us isolate several positive clones, which were identified to encode the full-length cDNA of the Smad3 gene. It was demonstrated that Smad3 could bind to NS5ATP9 in yeast cells (Supporting Fig. S2).

To further identify NS5ATP9 as a Smad3-interacting protein, the interaction between endogenous NS5ATP9 and Smad3 within cells such as LX-2, L02, and HepG2 cells was examined using co-IP assays. The Smad3 signal was detected in NS5ATP9 co-immunoprecipitation complexes, but no signal was detected in the control samples (Fig. 6a).

The potential colocalization of NS5ATP9 and Smad3 in LX-2 cells was examined via immunofluorescence imaging with confocal microscopy. Smad3 was observed predominantly in the cytoplasm and NS5ATP9 was localized in the cytoplasm and the nucleus (Fig. 6b, a. and b.). Furthermore, Smad3 exhibited excellent colocalization with NS5ATP9 (Fig. 6b, a.). As shown in Fig. 6b, b. and c., the silencing of NS5ATP9 markedly increased the Smad3 punctate and its nuclear expression (indicated by the arrow). Cytoplasmic expression of NS5ATP9 markedly increased upon TGF-β1 stimulation for 24 h (Fig. 6b, d. and e.), which was consistent with the results of western blotting (Fig. 1d). Following TGF-β1 stimulation, Smad3 expression decreased in cytoplasm but increased in nucleus (Fig. 6b, f. and g.).

DISCUSSION

Liver fibrosis is a pathological process of ECM excessive deposition, which is due to an imbalance between the production and degradation of matrix. HSCs have been widely acknowledged as the primary effector cells acting as the main origin of ECM [25–27]. In recent years,

Fig. 5. NS5ATP9 inhibited basal Smad3/p-Smad3 expression and abrogated TGF-β1-mediated p-Smad3 increase in LX-2 cells. LX-2 cells were transfected transiently with pcDNA 3.1/myc-His(−)-NS5ATP9 plasmid or siRNA-NS5ATP9 for 48 h. pcDNA3.1/myc-His(−)-NC and siRNA-NC were used as the respective negative controls, and the non-transfected LX-2 cells were used as the blank control. **a** Real-time PCR analysis showed that the levels of Smad3 and p-Smad3 mRNA were significantly downregulated by NS5ATP9 overexpression, **b** while they were significantly upregulated after NS5ATP9 silencing. **c** The protein expression levels of Smad3 and p-Smad3 decreased dramatically after LX-2 cells were induced to express NS5ATP9, while they increased after NS5ATP9 silencing. Also, after 24 h of transfection of cells according to the above method, the medium was replaced with serum-free medium in the presence or absence of TGF-β1 (5 ng/mL) and the cells were incubated for an additional 24 h before harvesting. **d**, **e** The levels of Smad3 and p-Smad3 were measured by western blotting. β-Actin was used as the internal control in real-time PCR. The quantitative ratios are shown as relative optical densities of the bands normalized to GAPDH expression. The western blotting data were quantified by using Bio1D software (VILBER, S:11.640150, France). The results shown are mean±SD. All assays were performed in triplicates. *$P<0.05$, **$P<0.01$.

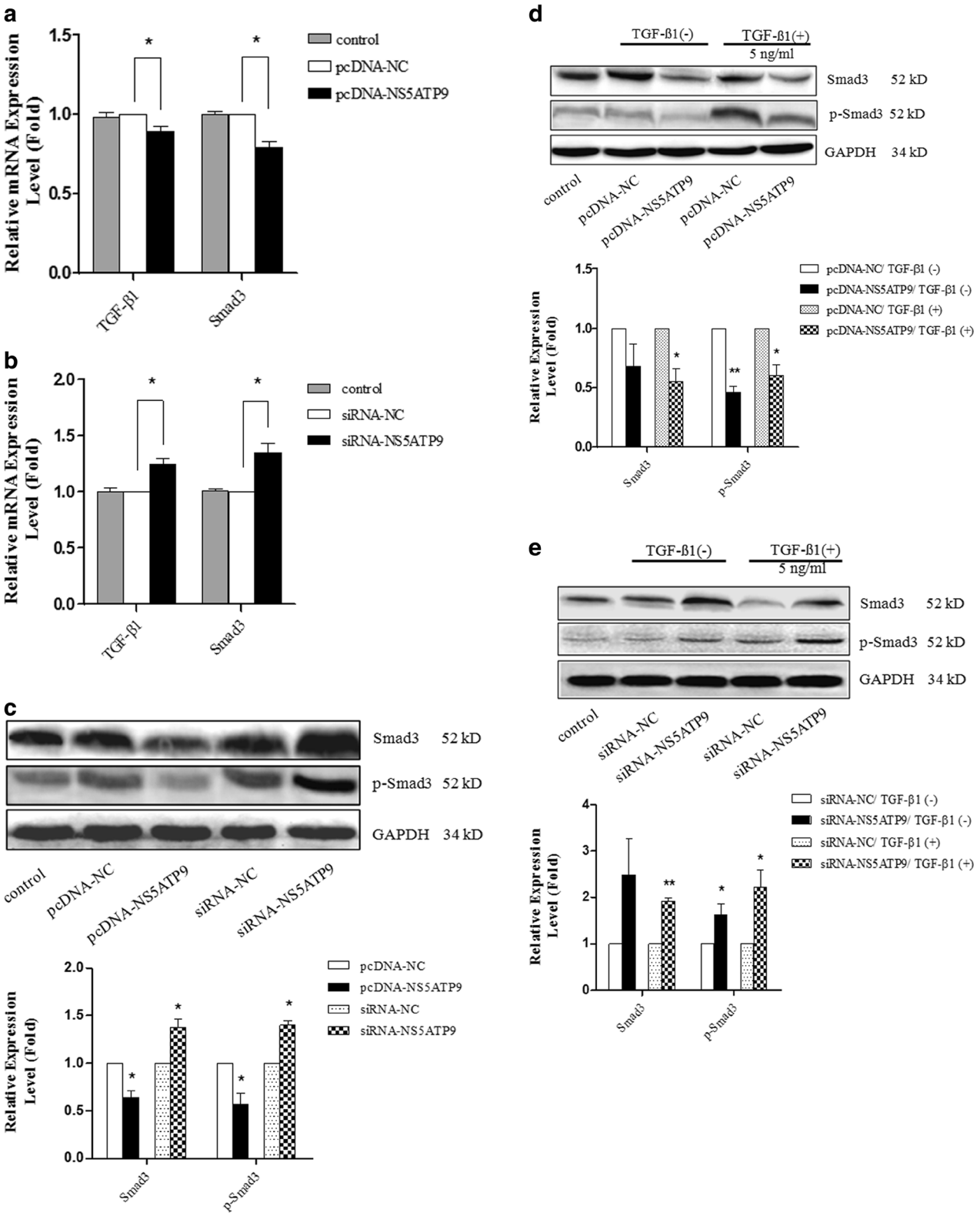
a
Relative mRNA Expression Level (Fold)
1.5
1.0
0.5
0.0
control
pcDNA-NC
pcDNA-NS5ATP9
TGF-β1
Smad3
b
Relative mRNA Expression Level (Fold)
2.0
1.5
1.0
0.5
0.0
control
siRNA-NC
siRNA-NS5ATP9
TGF-β1
Smad3
c
Smad3 52 kD
p-Smad3 52 kD
GAPDH 34 kD
control
pcDNA-NC
pcDNA-NS5ATP9
siRNA-NC
siRNA-NS5ATP9
Relative Expression Level (Fold)
2.0
1.5
1.0
0.5
0.0
pcDNA-NC
pcDNA-NS5ATP9
siRNA-NC
siRNA-NS5ATP9
Smad3
p-Smad3
d
TGF-ß1(-)
TGF-ß1(+)
5 ng/ml
Smad3 52 kD
p-Smad3 52 kD
GAPDH 34 kD
control
pcDNA-NC
pcDNA-NS5ATP9
pcDNA-NC
pcDNA-NS5ATP9
Relative Expression Level (Fold)
1.5
1.0
0.5
0.0
pcDNA-NC/ TGF-β1 (-)
pcDNA-NS5ATP9/ TGF-β1 (-)
pcDNA-NC/ TGF-β1 (+)
pcDNA-NS5ATP9/ TGF-β1 (+)
Smad3
p-Smad3
e
TGF-ß1(-)
TGF-ß1(+)
5 ng/ml
Smad3 52 kD
p-Smad3 52 kD
GAPDH 34 kD
control
siRNA-NC
siRNA-NS5ATP9
siRNA-NC
siRNA-NS5ATP9
Relative Expression Level (Fold)
4
3
2
1
0
siRNA-NC/ TGF-β1 (-)
siRNA-NS5ATP9/ TGF-β1 (-)
siRNA-NC/ TGF-β1 (+)
siRNA-NS5ATP9/ TGF-β1 (+)
Smad3
p-Smad3

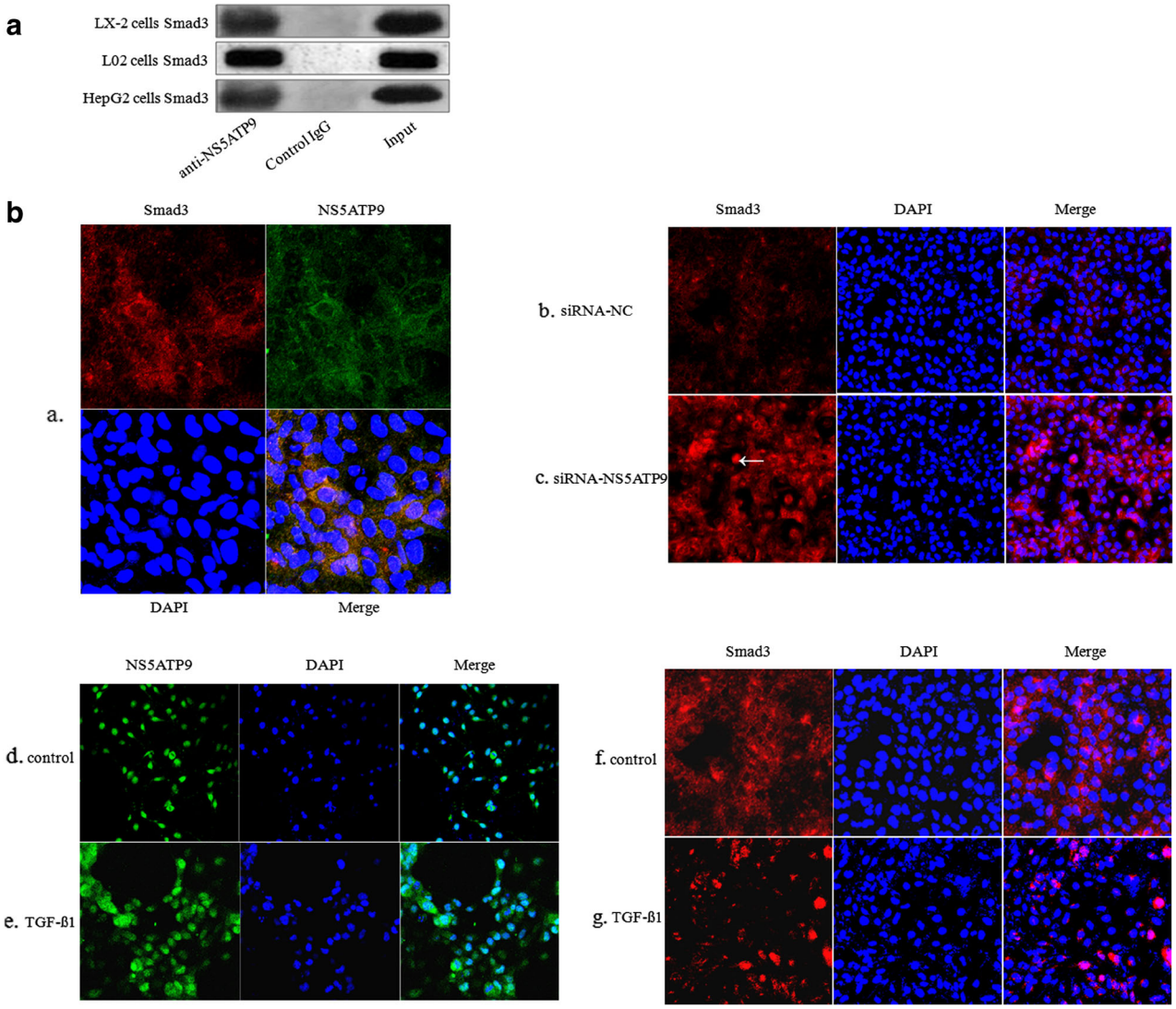

Fig. 6. NS5ATP9 interacted with Smad3 in LX-2 cells. **a** Anti-Smad3 western blotting of LX-2 cells, L02 cells, and HepG2 cells lysates following immunoprecipitation with the antibodies indicated at the bottom. **b** Confocal microscopy images displayed the subcellular localization of Smad3 (*red*) and NS5ATP9 (*green*) in merged image panels. The nuclei were stained with 4′,6-diamidino-2-phenylindole (DAPI; *blue*). **a.** Smad3 exhibited excellent colocalization with NS5ATP9 in the native LX-2 cells (×400). **b.**, **c.** The nuclear localization of Smad3 (indicated by the *arrows*) was enhanced in NS5ATP9-silenced LX-2 cells compared to the negative control cells (×200). **d.**, **e.** Cytoplasmic expression of NS5ATP9 was significantly higher after stimulation with TGF-β1 compared to the control (×200) (LX-2 cells were maintained in serum-free medium in the presence or absence of TGF-β1 (5 ng/mL) stimulation for 24 h). **f.**, **g.** Cytoplasmic expression of Smad3 decreased, but the nuclear expression increased after stimulation for 24 h with TGF-β1 compared to the control (×200).

NS5ATP9 is reported to be involved in many types of human cancers. Our previous study found that NS5ATP9 might play a role in the pathogenesis of HCV-associated HCC [8]. However, few studies reported on the correlation between NS5ATP9 and HSC activation. Here, to prove whether NS5ATP9 plays a role in HSC activation, we selected an immortalized human HSC line, LX-2 cells, as the cell model *in vitro*, which retains key features of activated HSC.

In this study, we found that NS5ATP9 did also express in LX-2 cells. Also, our results showed that NS5ATP9 overexpression significantly decreased the basal expression of the marker of HSC activation (α-SMA), collagen synthesis (COL I and COL III contribute the most to ECM accumulation in liver fibrosis) at both mRNA and protein levels in LX-2 cells. Inversely, NS5ATP9 silencing dramatically increased the expression of these genes,

providing the evidence that NS5ATP9 can inhibit HSC activation *in vitro*. Furthermore, NS5ATP9 overexpression abrogated the TGF-β1-induced increase in α-SMA and collagen production, whereas NS5ATP9 silencing coordinated with TGF-β1 to further promote LX-2 cells activation.

However, we also found that when LX-2 cells were exposed to TGF-β1, which is known for its profibrogenic and proproliferative effects on HSCs, endogenous NS5ATP9 expression significantly increased. We hypothesized that the increase of NS5ATP9 expression was a compensatory response of LX-2 cells after TGF-β1 stimulation. It could partially antagonize the effects of TGF-β1 to LX-2 cells. However, the antagonism of endogenous NS5ATP9 may be not sufficient to inhibit further activation of LX-2 cells.

Moreover, we proved that NS5ATP9 prevented LX-2 cells from proliferation and migration, and promoted apoptosis, which differs entirely from its proliferative and anti-apoptotic activities in most types of tumor cells [10, 14, 28, 29], but is consistent with that in others, including HCC [30, 31]. The promotion/suppression effects of NS5ATP9 on HSC apoptosis/proliferation may be one of the ways to protect HSCs from maintaining the activation status. To our knowledge, the present study is the first to show that NS5ATP9 can accelerate activated HSC apoptosis and inhibit migration. How could NS5ATP9 have the dual function of exerting either pro-apoptotic or anti-apoptotic effects in different cell types? One potential interpretation is that the expression and function of NS5ATP9 differ in diverse tissues and cell types.

On the other hand, Smad3 is a key signal transducer of TGF-β and directly involves in the regulation of HSC activation. We also found that NS5ATP9 lessened the expression of Smad3 and p-Smad3 and decreased the mRNA expression of TGF-β1, raising the possibility that NS5ATP9 may directly or indirectly participate in the negative regulation of the TGF-β1/Smad3 signaling pathway in activated HSC.

Yeast two-hybrid and co-IP assays showed that the physical complex between NS5ATP9 and Smad3 existed indeed in LX-2, L02, and HepG2 cells. This may be the molecular basis of NS5ATP9-regulated TGF-β1/Smad3 signaling pathway. Besides, we observed the colocalization of NS5ATP9 and Smad3 in LX-2 cells, which again proved their interaction. NS5ATP9 localizes to the cell plasma and nucleus, which is consistent with the results of a previous study [32], and Smad3 expresses mainly in the cytoplasm. Knockdown of NS5ATP9 could markedly increase nuclear accumulation of Smad3. This phenomenon indicated that NS5ATP9 might inhibit the phosphorylation of Smad3. Meanwhile, we observed that NS5ATP9 translocated into nucleus after starvation (LX-2 cells were maintained in the serum-free medium for 24 h) (as shown in Fig. 6b, a. and d.). According to the results of the previous study [14], NS5ATP9 was involved in the regulation of DNA repair after cell damage. Therefore, we speculate that starvation condition may cause NS5ATP9 nuclear translocation to participate in regulating cell damage repair. We will continue to further explore the function of NS5ATP9 in the cell damage caused by starvation.

Thus, these results revealed that NS5ATP9 could inhibit LX-2 cells activation and maintain their relative static state and suppress ECM deposition under both basal and TGF-β1-induced conditions, which may be achieved by reducing Smad3 expression, accordingly indirectly downregulating p-Smad3 or by directly inhibiting Smad3 phosphorylation. However, how NS5ATP9 participates in the regulation of the biological effects mediated by the TGF-β1/Smad3 signaling pathway is not clearly understood. Also, we cannot rule out the possibility that there is also some interaction between NS5ATP9 and another Smad family member. Therefore, future studies are necessary to identify the mechanism underlying the effect of NS5ATP9 on TGF-β1/Smad3 signaling pathway of HSC activation. In addition, whether these results and conclusions are applicable *in vivo* needs further verification. Therefore, it is indispensable to characterize the functional role of NS5ATP9 on animal models of liver fibrosis.

Our results largely extend the biological functions of NS5ATP9 in HSC activation, proliferation, migration, and apoptosis *in vitro*, suggesting that NS5ATP9 could suppress basal and TGF-β1-induced LX-2 cell activation and ECM production, possibly by suppressing Smad3/p-Smad3 expression.

ACKNOWLEDGMENTS

We thank Hongshan Wei and Guoli Li, Beijing Key Laboratory of Emerging Infectious Diseases; Dkewr Peng Wang, Liang Zhang, Lei Sun, and Xingang Zhou, Department of Pathology, Beijing Ditan Hospital, Capital Medical University; and Dr. Min Li, Department of Infectious Disease, the First Affiliated Hospital of Lanzhou University, for the supportive discussions and technical assistance.

Conflict of Interest. The authors declare no conflicts of interest related to this work.

Financial Support. This work was supported by grants from the National Natural Science Foundation of China (nos. 81470863), the Healthy Talent Leadership Programs of Beijing (nos. 2009-1-09), and the National Key Subjects Foundation of Infectious Diseases during the Five-Year Plan Period of China (nos. 2012ZX10002003, 2013ZX10002005, and 2012ZX10004904).

REFERENCES

1. Bataller, R., and D.A. Brenner. 2005. Liver fibrosis. *Journal of Clinical Investigation* 115: 209–218.
2. Mahato, R.I., K. Cheng, and R.V. Guntaka. 2005. Modulation of gene expression by antisense and antigene oligodeoxynucleotides and small interfering RNA. *Expert Opinion on Drug Delivery* 2: 3–28.
3. Friedman, S.L. 2008. Mechanisms of hepatic fibrogenesis. *Gastroenterology* 134: 1655–1669.
4. Inagaki, Y., and I. Okazaki. 2007. Emerging insights into transforming growth factor beta Smad signal in hepatic fibrogenesis. *Gut* 56: 284–292.
5. Piek, E., C.H. Heldin, and D.P. Ten. 1999. Specificity, diversity, and regulation in TGF-beta superfamily signaling. *FASEB Journal* 13: 2105–2124.
6. Massague, J. 2000. How cells read TGF-beta signals. *Nature Reviews Molecular Cell Biology* 1: 169–178.
7. Yu, P., B. Huang, M. Shen, et al. 2001. p15(PAF), a novel PCNA associated factor with increased expression in tumor tissues. *Oncogene* 20: 484–489.
8. Shi, L., S.L. Zhang, K. Li, et al. 2008. NS5ATP9, a gene up-regulated by HCV NS5A protein. *Cancer Letters* 259: 192–197.
9. Kato, T., Y. Daigo, M. Aragaki, K. Ishikawa, M. Sato, and M. Kaji. 2012. Overexpression of KIAA0101 predicts poor prognosis in primary lung cancer patients. *Lung Cancer* 75: 110–118.
10. Liu, L., X. Chen, S. Xie, C. Zhang, Z. Qiu, and F. Zhu. 2012. Variant 1 of KIAA0101, overexpressed in hepatocellular carcinoma, prevents doxorubicin-induced apoptosis by inhibiting p53 activation. *Hepatology* 56: 1760–1769.
11. Li, K., Q. Ma, L. Shi, et al. 2008. NS5ATP9 gene regulated by NF-kappaB signal pathway. *Archives of Biochemistry and Biophysics* 479: 15–9.
12. Mizutani, K., M. Onda, S. Asaka, et al. 2005. Overexpressed in anaplastic thyroid carcinoma-1 (OEATC-1) as a novel gene responsible for anaplastic thyroid carcinoma. *Cancer* 103: 1785–1790.
13. Yuan, R.H., Y.M. Jeng, H.W. Pan, et al. 2007. Overexpression of KIAA0101 predicts high stage, early tumor recurrence, and poor prognosis of hepatocellular carcinoma. *Clinical Cancer Research* 13: 5368–5376.
14. Emanuele, M.J., A. Ciccia, A.E. Elia, and S.J. Elledge. 2011. Proliferating cell nuclear antigen (PCNA)-associated KIAA0101/PAF15 protein is a cell cycle-regulated anaphase-promoting complex/cyclosome substrate. *Proceedings of the National Academy of Sciences of the United States of America* 108: 9845–9850.
15. Turchi, L., M. Fareh, E. Aberdam, et al. 2009. ATF3 and p15PAF are novel gatekeepers of genomic integrity upon UV stress. *Cell Death and Differentiation* 16: 728–737.
16. Quan M, Liu S, Li G, et al. 2013. A functional role for NS5ATP9 in the induction of HCV NS5A-mediated autophagy. *J Viral Hepat*, accepted.
17. Xu, L., A.Y. Hui, E. Albanis, et al. 2005. Human hepatic stellate cell lines, LX-1 and LX-2: new tools for analysis of hepatic fibrosis. *Gut* 54: 142–151.
18. Chen, Y.L., J. Lv, X.L. Ye, et al. 2011. Sorafenib inhibits transforming growth factor beta1-mediated epithelial–mesenchymal transition and apoptosis in mouse hepatocytes. *Hepatology* 53: 1708–1718.
19. Xiao, X., Y. Gang, Y. Gu, et al. 2012. Osteopontin contributes to TGF-beta1 mediated hepatic stellate cell activation. *Digestive Diseases and Sciences* 57: 2883–2891.
20. Shimada, H., N.R. Staten, and L.E. Rajagopalan. 2011. TGF-beta1 mediated activation of Rho kinase induces TGF-beta2 and endothelin-1 expression in human hepatic stellate cells. *Journal of Hepatology* 54: 521–528.
21. Lim, J.Y., M.A. Oh, W.H. Kim, H.Y. Sohn, and S.I. Park. 2012. AMP-activated protein kinase inhibits TGF-beta-induced fibrogenic responses of hepatic stellate cells by targeting transcriptional coactivator p300. *Journal of Cellular Physiology* 227: 1081–1089.
22. Krizhanovsky, V., M. Yon, R.A. Dickins, et al. 2008. Senescence of activated stellate cells limits liver fibrosis. *Cell* 134: 657–667.
23. Shi, Y., and J. Massague. 2003. Mechanisms of TGF-beta signaling from cell membrane to the nucleus. *Cell* 113: 685–700.
24. Massague, J., and Y.G. Chen. 2000. Controlling TGF-beta signaling. *Genes and Development* 14: 627–644.
25. Jiao, J., S.L. Friedman, and C. Aloman. 2009. Hepatic fibrosis. *Current Opinion in Gastroenterology* 25: 223–229.
26. Lotersztajn, S., B. Julien, F. Teixeira-Clerc, P. Grenard, and A. Mallat. 2005. Hepatic fibrosis: molecular mechanisms and drug targets. *Annual Review of Pharmacology and Toxicology* 45: 605–628.
27. Friedman, S.L. 2008. Hepatic fibrosis—overview. *Toxicology* 254: 120–129.
28. Jain, M., L. Zhang, E.E. Patterson, and E. Kebebew. 2011. KIAA0101 is overexpressed, and promotes growth and invasion in adrenal cancer. *PLoS ONE* 6: e26866.
29. Hosokawa, M., A. Takehara, K. Matsuda, et al. 2007. Oncogenic role of KIAA0101 interacting with proliferating cell nuclear antigen in pancreatic cancer. *Cancer Research* 67: 2568–2576.
30. Guo, M., J. Li, D. Wan, and J. Gu. 2006. KIAA0101 (OEACT-1), an expressionally down-regulated and growth-inhibitory gene in human hepatocellular carcinoma. *BMC Cancer* 6: 109.
31. Wang, Q., Y. Wang, Y. Li, X. Gao, S. Liu, and J. Cheng. 2013. NS5ATP9 contributes to inhibition of cell proliferation by hepatitis C virus (HCV) nonstructural protein 5A (NS5A) via MEK/extracellular signal regulated kinase (ERK) pathway. *International Journal of Molecular Sciences* 14: 10539–10551.
32. Simpson, F., K.L. Lammerts van Bueren, N. Butterfield, et al. 2006. The PCNA-associated factor KIAA0101/p15(PAF) binds the potential tumor suppressor product p33ING1b. *Experimental Cell Research* 312: 73–85.